

# Separation of sources and 3D inversion of gravity and magnetic data for the Thuringian Basin, Germany

Ilya PRUTKIN<sup>1</sup>, Gerhard JENTZSCH<sup>1</sup>, Thomas JAHR<sup>1</sup>

<sup>1</sup> Institute of Earth Sciences, Jena University

Burgweg 11, 07749 Jena, Germany; e-mail: Ilya.Prutkin@uni-jena.de

**Abstract:** We propose a novel methodology for separation of potential field sources and its 3D inversion. New approaches are developed to separate sources: i) in depth using a succession of upward and downward continuation; ii) in the lateral direction by means of approximation with the field of 3D line segments; iii) according to density and magnetization contrast based on pseudo-gravity calculation. Our original inversion algorithms allow the recovery of unknown 3D geometry both for a restricted body of arbitrary shape and for a contact surface. For the first time, we apply our algorithms to joint inversion of gravity and magnetic data for a large area (the Thuringian Basin in central Germany). We separate in depth sources of both gravitational and magnetic anomalies for the whole territory of Thuringia and compare corresponding components. A 3D model of the main sources is presented based on approximation with 3D line segments and their further transforming into a restricted body or a contact surface with the same field.

**Key words:** potential field methods, 3D inversion, pseudo-gravity, sedimentary basin

## 1. Introduction

Our investigation is carried out under the framework of the project INFLUINS (Integrated Fluid Dynamics in Sedimentary Basins) devoted to the relationship between near surface and deeper fluids and material flows (*Kley et al., 2011*). The project links geology, hydrogeology, mineralogy, geophysics, basin analysis, remote sensing, etc. Geophysical investigation is necessary in order to explain the internal structure of the Thuringian Basin and to develop a joint 3D model of its underground using seismic, gravimetric, magnetic, borehole measurements. In our paper we present results on 3D inversion of gravity and magnetic data.

The Thuringian Basin is bordered in the north by the Harz mountains, in the south by the Thuringian Forest mountains and in the east by the Thuringian slate belt. Geologically, it contains sandstones, limestones, clays, gypsum and salt, which were deposited from the late Permian to the earliest Jurassic (approximately 250 to 180 million years ago). The largest deposits are of Triassic age. The present day basin geometry developed more recently, when, 80 million years ago, the African and European tectonic plates collided with one another. The Thuringian basin began to subside at this time, whilst the surrounding regions were squeezed together. More details about geology of the area can be found in *Behr et al. (1984)*. For the part of the area we refer to the gravitational modeling done by *Gabriel (1997)*.

Our new methodology for 3D potential field data inversion has been tested in *Prutkin et al. (2011)* on a local isolated gravitational anomaly. In this paper, we process both gravity and magnetic data for a bigger area. Each field represents a complex composition of various signals. We begin with separation in depth of both gravitational and magnetic anomalies for the whole area of Thuringia. We separate sources into shallow, intermediate and deep ones. Their comparison reveals that anomalies are caused partly by different objects.

We demonstrate all steps of our methodology on a local anomaly caused by one of the intermediate sources. First, we subtract a model of the regional field. Then, we approximate the residual anomaly by the field of several 3D line segments. At last, we apply our inversion algorithms to transform segments into a 3D restricted body, which is interpreted geologically as a granitic intrusion. It is also possible, to invert gravity data for a contact surface. This is shown for another anomaly, where the same steps provides 3D topography of a density contrast interface. We join both solutions and obtain a 3D model for the main intermediate sources.

The most noticeable anomaly caused by shallow sources is an arc-shaped anomaly presented both in gravity and magnetic data. To prove that both anomalies are generated by the same source, we calculate pseudo-gravity from magnetic data and study its correlation with the given gravity. Inversion of magnetic data provides 3D topography for an uplift of the crystalline. Its gravitational effect is subtracted from measured gravity. The rest of gravity is attributed to topography of near-surface layers. All ob-

tained objects (the intrusion, uplifts of the deep contact and crystalline, near-surface layers) form an initial approximation for IGMAS (*Götze and Lahmeyer, 1988*). By means of this software for direct modeling we obtain a more detailed geological section incorporating both geological information and results of other geophysical methods.

The paper is organized as following: we present our new algorithms for separation of sources and for 3D gravity and magnetic data inversion, then the algorithms are applied to interpretation of measurements for the Thuringian Basin. In Section 2, we start with the algorithm to isolate sources in depth. After separation of sources for the whole area, we take a local anomaly and show results of its approximation with the field of 3D line segments in the same section. In Section 3, the method of local corrections for 3D potential field data inversion is introduced, as well as our new integral equations for gravitational and magnetic inverse problems. A 3D model for the main intermediate sources and interpretation of the arc-shaped anomaly are presented in Section 4. Section 5 contains the main conclusions of our study.

## 2. Separation of sources

We use the Bouguer anomaly data in gravity modeling and total magnetic intensity anomaly in our magnetic investigation. Both data sets represent gridded data for the whole area of Thuringia, grid distance is 500 m. First, we apply our algorithm for separation of sources in depth based on upward and downward continuation (*Prutkin and Casten, 2009*). Our goal is to find a part of the observed field which is harmonic above a given depth  $h$ . Integration along the area of investigation only is possible due to subtraction of a model of the regional field prior to the upward continuation, which we treat as 2D harmonic function. We apply the algorithm to both gravity and magnetic data for the whole area of Thuringia and separate sources into shallow (above 5 km), intermediate (between 5 and 20 km) and deep ones (below 20 km). Their comparison reveals that gravitational and magnetic anomalies are caused partly by different objects. For instance, a component of gravity corresponding to deep sources is caused mainly by an uplift of Moho, meanwhile the same component of the magnetic field is generated by

the Mid-German Crystalline High (see Fig. 1).

Separation of sources into shallow, intermediate and deep ones deals with the depth to singularities of the corresponding component as a harmonic function. Of course, an effect of smooth undulations of a density interface can be harmonic down to great depths. For instance, gravity of deep sources in Fig. 1 includes also a long-wave effect of the basin structure. On the other hand, shallow singularities can not belong to the field of deep objects.

We demonstrate all steps of our inversion methodology on a negative gravity anomaly, which belongs to the intermediate sources (see Fig. 2). First, we subtract a model of the regional field. The model (2D harmonic function with the same values on the boundary as the given data) is shown in Fig. 2 (bottom). After subtracting the regional field, we obtain the residual anomaly (Fig. 3, top), which is an object of further processing.

Approximation by the field of several 3D line segments not only separates sources in the lateral direction, but also provides reliable estimates of their masses and depths. The effect of a line segment can be evaluated by a quite simple formula (Prutkin *et al.*, 2011). It is a considerably flexible tool for the approximation of the observed data. We approximate the chosen anomaly with a field of several 3D line segments. Two line segments are sufficient for fairly accurate approximation of the given data. The RMS of differences between the observed data and the field of the line segments is 0.41 mGal. The field of 3D line segments is presented in Fig. 3 (bottom).

To check if both gravitational and magnetic anomalies are caused by the same object, we calculate pseudo-gravity from magnetic data and compare it with the observed gravity. We apply our own original approach for transformation of magnetic data to pseudo-gravity. We assume that given data is harmonic above some horizontal plane located below the Earth's surface. We introduce a Cartesian coordinate system where this plane coincides with the coordinate plane  $xOy$ . Then the vertical derivative of the gravitational potential  $V_z$  everywhere above the plane can be evaluated by means of the Poisson's integral:

$$V_z(x, y, z) = \frac{1}{2\pi} \iint P(x, y, z, x', y') V_z(x', y', 0) dx' dy', \quad (1)$$

$P(x, y, z, x', y') = z / ((x - x')^2 + (y - y')^2 + z^2)^{3/2}$ . According to the Poisson's relation, for the vertical component  $H_z$  of the magnetic field intensity we have:

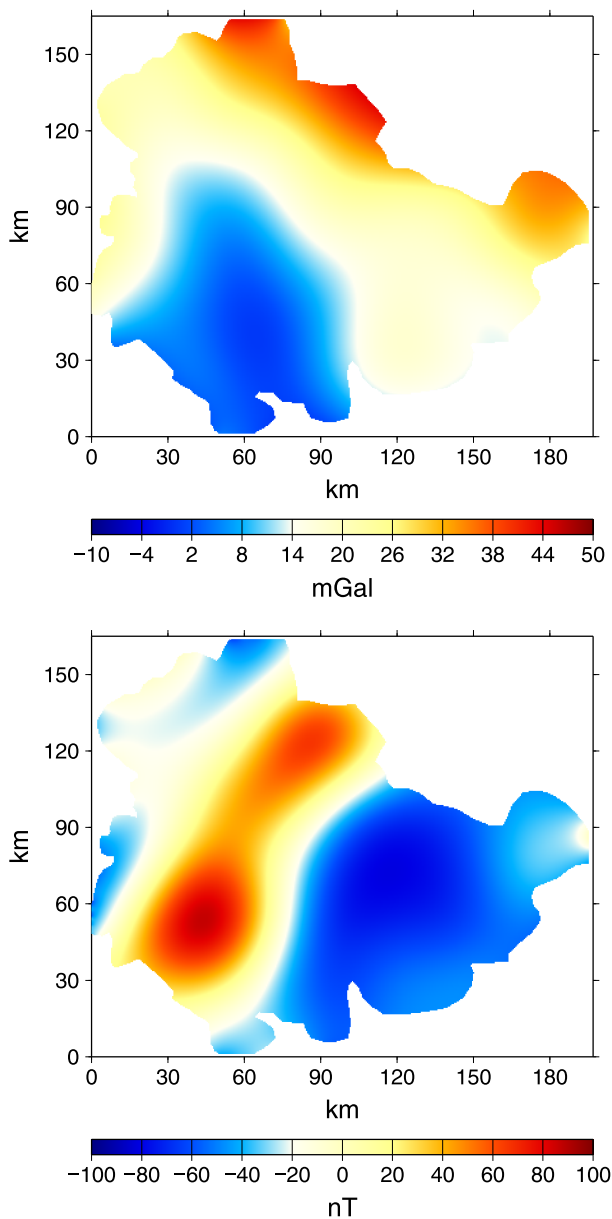


Fig. 1. Comparison of gravitational and magnetic effects from deep sources. Top – gravity, bottom – magnetic field.

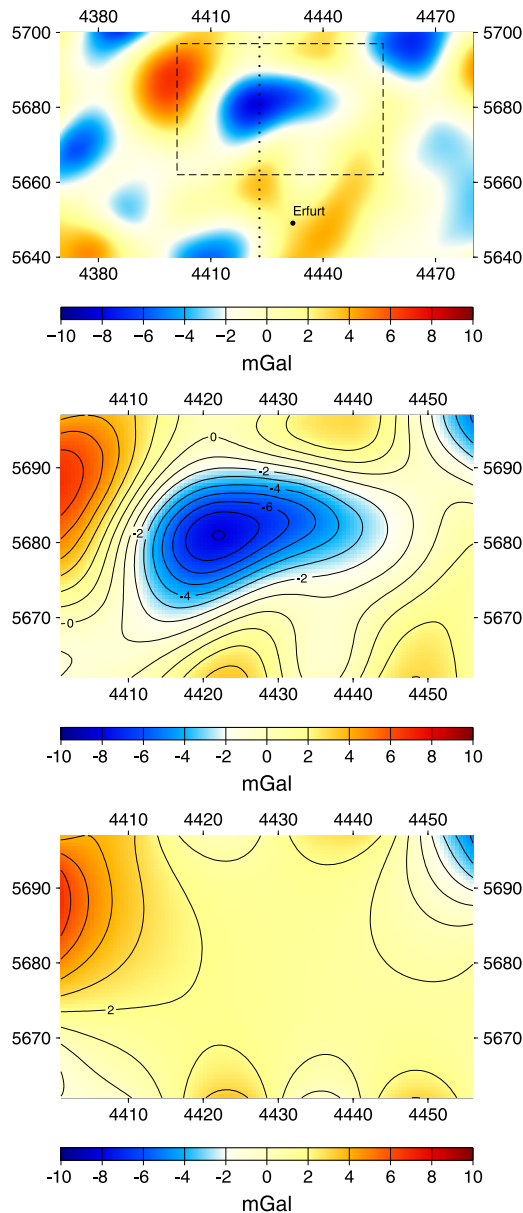


Fig. 2. Local negative anomaly. Top – its location (dotted line – IGMAS section), middle – zoomed anomaly, bottom – suggested model of regional field (2D harmonic function). Gauss-Krüger coordinates are used (in km).

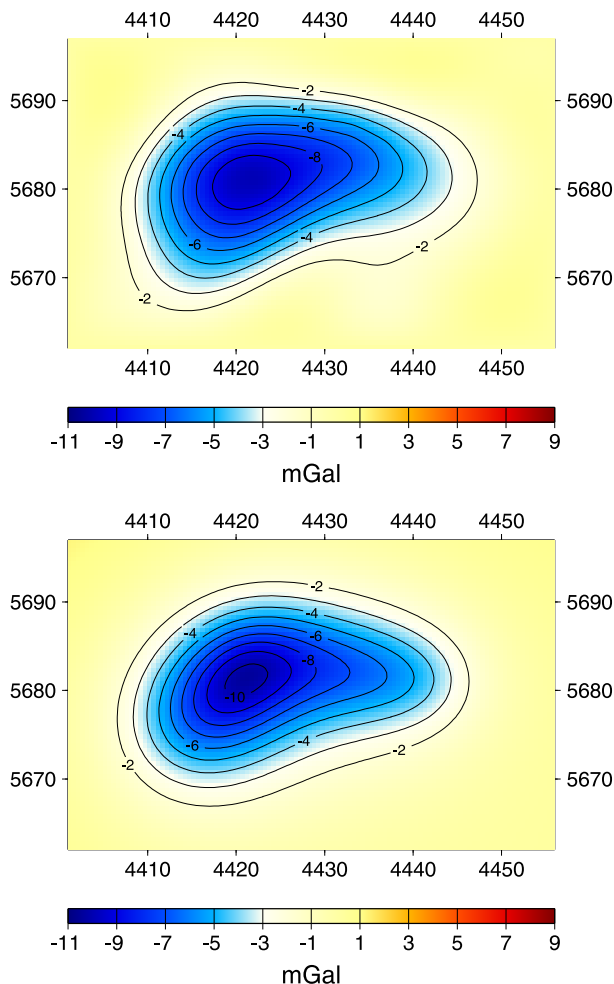


Fig. 3. Approximation of the negative anomaly with line segments. Top – observed data after subtracting the model regional field; bottom – gravitational effect of two line segments. The RMS of residuals is 0.41 mGal.

$$H_z = M_x V_{xz} + M_y V_{yz} + M_z V_{zz} , \quad (2)$$

where  $M_x$ ,  $M_y$  and  $M_z$  are components of magnetization. We apply to both sides of Eq. (1) a linear differential operator  $M_x \frac{\partial}{\partial x} + M_y \frac{\partial}{\partial y} + M_z \frac{\partial}{\partial z}$ . Using (1) and (2), we obtain

$$H_z(x, y, z) = \frac{1}{2\pi} \iint K_1(x, y, z, x', y') V_z(x', y', 0) dx' dy' , \quad (3)$$

where

$$K_1(x, y, z, x', y') = \frac{-3z(x - x')M_x - 3z(y - y')M_y + ((x - x')^2 + (y - y')^2 - 2z^2)M_z}{((x - x')^2 + (y - y')^2 + z^2)^{5/2}} . \quad (4)$$

For total magnetic intensity anomaly

$$\Delta T = |\mathbf{F} + \Delta \mathbf{F}| - |\mathbf{F}|, \quad (5)$$

where  $\mathbf{F}$  is the main geomagnetic field,  $\Delta \mathbf{F}$  is the anomalous magnetic field, the following approximation is valid (*Blakely, 1995*):

$$\Delta T \approx \frac{1}{|\mathbf{F}|} \mathbf{F} \cdot \Delta \mathbf{F} . \quad (6)$$

We introduce a unit vector directed along the main geomagnetic field:

$$\mathbf{e} = (e_x, e_y, e_z) = \frac{1}{|\mathbf{F}|} \mathbf{F} . \quad (7)$$

From (6) and the Poisson's relation we obtain

$$\begin{aligned} \Delta T &= \mathbf{e} \cdot \Delta \mathbf{F} = e_x H_x + e_y H_y + e_z H_z = \\ &= e_x (M_x V_{xx} + M_y V_{xy} + M_z V_{xz}) + e_y (M_x V_{xy} + M_y V_{yy} + \\ &+ M_z V_{yz}) + e_z (M_x V_{xz} + M_y V_{yz} + M_z V_{zz}) . \end{aligned} \quad (8)$$

Assume that the gravitational potential on the Earth's surface is approximated by a simple layer integral with unknown density  $\mu(x, y, 0)$  distributed on the plane  $z = 0$  below the surface:

$$V(x, y, z) = -\frac{1}{2\pi} \iint \frac{\mu(x', y', 0)}{((x - x')^2 + (y - y')^2 + z^2)^{1/2}} dx' dy' . \quad (9)$$

We take the vertical derivative of both sides of (9). It reveals that the unknown function  $\mu(x, y, 0)$  satisfies the same integral equation (1) as  $V_z(x, y, 0)$ . Differentiating both sides of (9) provides all second derivatives we need in (8). We substitute in these expressions  $V_z$  instead of  $\mu$  and from (8) deduce an equation similar to (3), but with a bit more complex kernel



$$\Delta T(x, y, z) = \frac{1}{2\pi} \iint K_2(x, y, z, x', y') V_z(x', y', 0) dx' dy' , \quad (10)$$

where

$$\begin{aligned} K_2(x, y, z, x', y') = & e_x \frac{((y-y')^2 + z^2 - 2(x-x')^2)M_x - 3(x-x')(y-y')M_y - 3z(x-x')M_z}{((x-x')^2 + (y-y')^2 + z^2)^{5/2}} + \\ & + e_y \frac{-3(x-x')(y-y')M_x + ((x-x')^2 + z^2 - 2(y-y')^2)M_y - 3z(y-y')M_z}{((x-x')^2 + (y-y')^2 + z^2)^{5/2}} + \\ & + e_z \frac{-3z(x-x')M_x - 3z(y-y')M_y + ((x-x')^2 + (y-y')^2 - 2z^2)M_z}{((x-x')^2 + (y-y')^2 + z^2)^{5/2}} . \end{aligned} \quad (11)$$

We can rewrite (11) with smaller number of terms. The assumption that magnetization is directed along the main geomagnetic field leads to its further simplification.

We treat formulas (3) and (10) as linear integral equations of the 1st kind: the magnetic field (its vertical component or total magnetic intensity) is given on the Earth's surface, we have to find from the corresponding equation the unknown function  $V_z(x, y, 0)$ . After the equation is solved, we calculate pseudo-gravity on the Earth's surface by means of the Poisson's integral (1).

### 3. Inversion algorithms

We reduce inversion problems both for a restricted body and for a contact surface to nonlinear integral equations of the 1st kind. In the case of a restricted object, we assume that the sought body is star convex relative to some interior point (for instance, relative to its center of mass). Then, we can introduce spherical coordinates  $r, \theta, \varphi$  relative to the point, the body boundary can be determined by the equation  $r = r(\theta, \varphi)$ , where  $r(\theta, \varphi)$  is a single-valued function. To find an unknown function  $r(\theta, \varphi)$ , we have to solve the following nonlinear integral equation:

$$G\Delta\sigma \iint K(x, y, z, \theta, \varphi, r(\theta, \varphi)) d\theta d\varphi = U(x, y, z) , \quad (12)$$

where  $G$  is the gravitational constant,  $\Delta\sigma$  is the density contrast,  $U(x, y, z)$  is the given field. For a fixed value of  $\Delta\sigma$ , the solution of the inverse problem is unique according to the Novikov's theorem (Novikov, 1938).

We have derived new integral equations of gravitational and magnetic inverse problems. As distinct from known equations, their integrands are algebraic relative to the function sought and do not contain its derivatives (Prutkin, 2008). As a function  $U$  in Eq. (12), we use a special combination of the gravitational potential and its derivatives. Based on the approximation of the observed field by the field of 3D line segments, this combination can be easily calculated.

In the case of a contact surface, we apply Cartesian coordinates. An unknown 3D topography is determined by the equation  $z = z(x, y)$ . We find an unknown function  $z(x, y)$  from the corresponding nonlinear integral equation of the 1st kind (Prutkin and Saleh, 2009). We can use gravity or magnetic data directly on the physical surface, approximation with 3D line segments is necessary only if we need to separate sources and estimate their depths.

We solve the integral equations relative to the functions  $r(\theta, \varphi)$  or  $z(x, y)$  by the original method of local corrections. Our method of inversion is of the same type, as the method of Cordell and Henderson (1968), a solution is calculated from data automatically by successive iterations. In each iteration an attempt is made to decrease the difference between the given and approximate field values at a fixed node only by means of a change in the value of the function sought at the same node. These considerations lead to decomposition of the inverse problem and reduction of time expenditures to solve it approximately by an order of magnitude.

#### 4. Model solutions for the geological section

After the separation of gravitational signals, we transform the formal sources used as anomalous sources approximation (3D line segments) into objects of more geological meaning. For a given set of segments we obtain a restricted body or a contact surface generating the same gravity.

Using our inversion algorithms described in the previous section, we transform two 3D line segments approximating the local negative anomaly

(see Fig. 2, 3) into a restricted body with the same gravity as the line segments (both with negative line density). The body is interpreted as a granitic intrusion in the denser ambient medium (crystalline). Then we repeat the same steps for a positive anomaly to the west of the negative one. Since approximation provides deeper sources, we attribute the anomaly to an uplift of a density interface below the body. We present a 3D model for the main intermediate sources in Fig. 4.

Due to non-uniqueness in geophysical inverse problems, there are various admissible solutions causing the same gravity. For instance, the negative anomaly can be explained by a depression of a density interface. In our interpretation we follow the geological concept of *Behr et al. (1984)* about crystalline rocks intruded by Variscan granites, as well as results of previous gravity modeling (*Gabriel, 1997*).

Among effects generated by near-surface objects, the most discernible is an arc-shaped anomaly, which bounds the Thuringian Basin from the west. The anomaly is clearly visible both in gravity and in magnetic data. First, we transform the magnetic anomaly into pseudo-gravity based on our original algorithms. Then, we compare the calculated pseudo-gravity with the measured gravity. Their correlation equals to 68.5%, it proves that both gravity and magnetic anomalies are likely caused by the same source. Since the anomaly is more recognizable in magnetic data, we invert the magnetic measurements for 3D topography of a contact surface. Depths to the magnetic interface vary from 1.4 to 2.4 km. The interface is assumed to be an uplift of crystalline. We calculate the gravitational effect of the magnetic topography and subtract it from the given gravity. After subtraction we obtain quite small gravity anomalies which are attributed to topography of the near-surface layers.

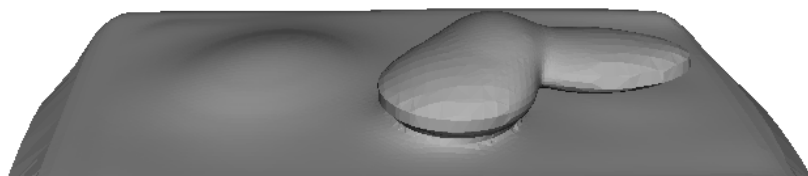


Fig. 4. Three-dimensional model for the main intermediate sources. It includes anomalous body above a density interface with an elevation to the west of the body.

We join all found objects (the granitic intrusion, the uplifts of the deep density interface and crystalline, near-surface layers) and obtain a 3D model which forms an initial approximation for IGMAS (*Götze and Lahmeyer, 1988*). This program suite for direct modeling allows taking into account both geological information and additional results of other geophysical methods (seismic, borehole data, etc.). A geological section along the south-north profile shown in Fig. 2 (top) is presented in Fig. 5. Recently a seismic profile was measured, located close to the section presented in Fig. 5. Its interpretation for shallow layers is in good agreement with our results.

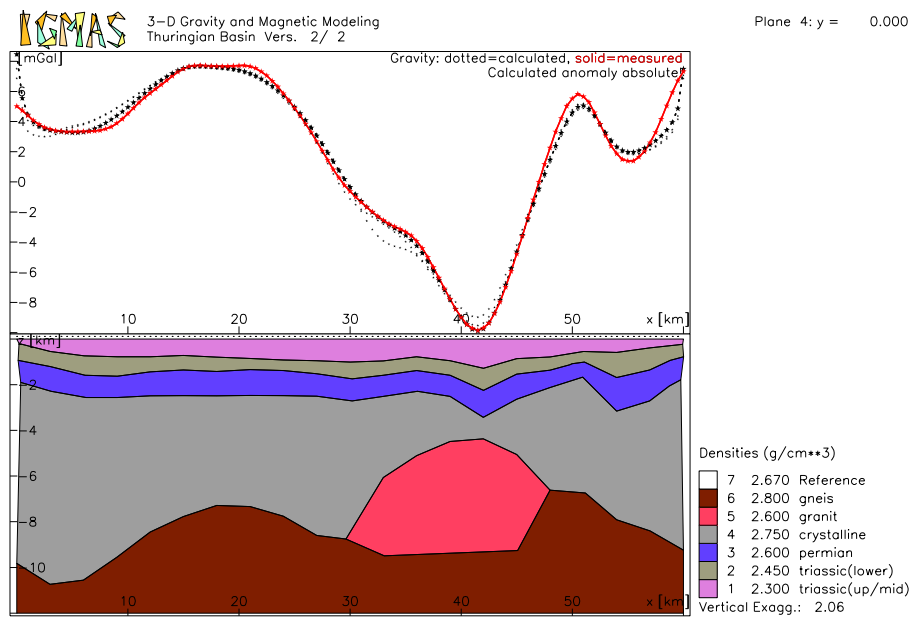


Fig. 5. Geological section: IGMAS modeling. It goes along the profile shown in Fig. 2 (top) and joins the granitic intrusion, uplifts of the deep density interface and crystalline, and near-surface layers.

5. Summary and conclusions

The following conclusions are drawn from the conducted investigation:

1. Our methodology for separation of sources and 3D inversion can be applied to both gravity and magnetic data for a big area. Based on up-

ward and downward continuation, we have separated in depth anomalous objects according to their gravitational and magnetic effects for the whole territory of Thuringia into shallow, intermediate and deep ones. We have compared corresponding components of gravity and magnetic field and observed that they are generated partly by different sources.

2. For each anomaly, its interpretation includes several steps. First, we subtract a model of the regional field, which satisfies 2D Laplace equation inside the investigation area and has the same values on its boundary as the given data. Then, we approximate the residual field by the field of 3D line segments. It provides separation in the lateral direction and reasonable estimates of mass and depth for an anomalous object. At last, we apply our inversion algorithms and obtain a restricted body or a contact surface with the same field as a chosen set of line segments. For two main intermediate anomalies, we have inverted data for an anomalous body (a granitic intrusion) and a density interface with topography below it.
3. We suggest an original algorithm to transform magnetic data to pseudo-gravity based on downward continuation. We compare the calculated pseudo-gravity with the measured gravitational field. Their high correlation indicates that both gravity and magnetic anomalies are likely caused by the same object. We have applied this approach to an arc-shaped anomaly presented both in gravity and magnetic data (shallow sources). Inversion of the magnetic anomaly provides 3D topography for an uplift of the crystalline.
4. All obtained objects are joined into a 3D model for the main shallow and intermediate sources. The model forms an initial approximation for IGMAS modeling. At this step, we refine the geological section and incorporate geological information and results of other geophysical methods. The next goal is a 3D model for the whole area of the Thuringian Basin.

**Acknowledgments.** Our investigation is carried out under the framework of the project INFLUINS funded by the German Federal Ministry of Education and Research (BMBF grant No. 03IS2091A). This support is gratefully acknowledged.

## References

- Behr H.-J., Engel W., Franke W., Giese P., Weber K., 1984: The Variscan Belt in Central Europe: main structures, geodynamic implications, open questions. *Tectonophys.*, **109**, 15–40.
- Blakely R. J., 1995: *Potential Theory in Gravity and Magnetic Applications*. Cambridge University Press, Cambridge, 441 p.
- Cordell L., Henderson R. G., 1968: Iterative three-dimensional solution of gravity anomaly data using a digital computer. *Geophys.*, **33**, 596–601.
- Gabriel G., 1997: *Der Harz und sein südliches Vorland: Interpretation der Bouguer–Anomalie und spezielle Studien zur Geodynamik mit der Methode der finiten Elemente*. Dissertation, TU Clausthal, 191 p.
- Götze H.-J., Lahmeyer B., 1988: Application of three-dimensional interactive modelling in gravity and magnetics. *Geophys.*, **53**, 1096–1108.
- Kley J., the INFLUINS team, 2011: INFLUINS: Investigating fluid flow between surface and deep levels of sedimentary basins: The Thuringian Basin as a geolaboratory. *Geophys. Res. Abstr.*, **13**, EGU2011–3005.
- Novikov P. S., 1938: Sur le problème inverse du potentiel. *Dokl. Akad. Nauk SSSR*, **18**, 165–168.
- Prutkin I., 2008: Gravitational and magnetic models of core – mantle boundary and their correlation. *J. Geodyn.*, **45**, 146–153.
- Prutkin I., Casten U., 2009: Efficient gravity data inversion for 3D topography of a contact surface with application to the Hellenic subduction zone. *Comput. & Geosci.*, **35**, 225–233.
- Prutkin I., Saleh A., 2009: Gravity and magnetic data inversion for 3D topography of the Moho discontinuity in the northern Red Sea area, Egypt. *J. Geodyn.*, **47**, 237–245.
- Prutkin I., Vajda P., Tenzer R., Bielik M., 2011: 3D inversion of gravity data by separation of sources and the method of local corrections: Kolarovo gravity high case study. *J. Appl. Geophys.*, **75**, 472–478.